X-ray absorption spectroscopy and x-ray magnetic circular dichroism simultaneous measurements under high pressure: the iron bcc–hcp transition case

2005 J. Phys.: Condens. Matter 17 S957

(http://iopscience.iop.org/0953-8984/17/11/028)

INSTITUTE OF PHYSICS PUBLISHING JOURNAL OF PHYSICS: CONDENSED MATTER

J. Phys.: Condens. Matter **17** (2005) S957–S966 doi:10.1088/0953-8984/17/11/028

X-ray absorption spectroscopy and x-ray magnetic circular dichroism simultaneous measurements under high pressure: the iron bcc–hcp transition case

F Baudelet[1,2], S Pascarelli[3], O Mathon[3], J P Itié[1], A Polian[1], M d' Astuto[1] and J C Chervin[1]

[1] Physique des Milieux Condensés, CNRS-UMR 7602, 140 rue de Lourmel, 75015 Paris, France
[2] Synchrotron SOLEIL, L'Orme des Merisiers, Saint-Aubin, BP 48, 91192, Gif-sur-Yvette Cedex, France
[3] European Synchrotron Radiation Facility, BP 220, 38043 Grenoble Cedex, France

Received 5 January 2005
Published 4 March 2005
Online at stacks.iop.org/JPhysCM/17/S957

Abstract

XAS (x-ray absorption spectroscopy) and XMCD (x-ray magnetic circular dichroism) studies performed simultaneously give the structural and the magnetic properties of the same compound in rigorously the same thermodynamic conditions. The high pressure iron bcc to hcp phase transition has been studied with these combined techniques. The magnetic and structural transitions are sharp. Both are of first order and they occur in the same pressure domain, as theoretically predicted. The pressure domain of the structural transition is found at around 2.4 ± 0.2 GPa, narrower than usually described in the literature. No room temperature ferromagnetic order has been found in the iron hcp phase close to the transition pressure. The magnetic transition occurs in a narrower domain and slightly precedes the structural one.

(Some figures in this article are in colour only in the electronic version)

1. Introduction

Polarized x-ray absorption contains intrinsic structural, electronic and magnetic probes: the x-ray absorption near edge structure (XANES) and extended x-ray absorption fine structure (EXAFS) profiles, which can be used to differentiate clearly the signatures of bcc and hcp ordering in 3d transition metals for example, and the x-ray magnetic circular dichroism (XMCD), which is very sensitive to polarized magnetic moment variation.

The XMCD signal at the K edge of iron is due to many contributions and mainly to the spin–orbit coupling in the final state (the 4p probed state) of the photoelectron. It is quite difficult to extract absolute quantitative information on the magnetic moment from XMCD at the K edges. The comparison between XMCD signals in different compounds can give

information about the magnetic orientations of the probed element relative to another one in the same compound, or about the variation of the magnetic moment of an element with temperature or with pressure. Different theoretical approaches for the interpretation of K edge XMCD signals lead to the same conclusion that the main contribution to these signals comes from the interaction of the excited 4p photoelectron with the spin-polarized 3d bands [1–3]. It is therefore natural to conclude that the integral of the XMCD signal at the K edge of iron is proportional to the 3d magnetic moment.

The iron phase diagram has attracted considerable interest for a long time. At the beginning, the motivation was provided by its central role in the understanding of the behaviour of alloys and steel and their production [4]. Its geophysical importance is also easily understood, because of its predominant abundance in the Earth' core [5, 6]. Iron metallurgy is one of the older scientific topics of research but the iron phase diagram at extreme pressure and temperature conditions is still far from being established. Under the application of an external pressure at ambient T, iron undergoes a transition at 13 GPa from the bcc α-phase to the hcp ε-phase structure [7], with the loss of its ferromagnetic long range order [8]. In the literature the transition extends over 8 GPa at ambient temperature; within it, the bcc and hcp phases coexist [9]. In the pure hcp ε-phase, superconductivity appears close to the transition between 15 and 30 GPa [10, 11]. The evolution of the magnetic state with pressure across this transition is a subject of current active research essentially based on Mössbauer measurements [8, 12–14] and recent work using inelastic x-ray scattering [15]. The authors report on the variation of a satellite in the Fe Kβ fluorescence line, which shows that the magnetic moment of iron decreases over the same pressure range as the bcc to hcp transition, i.e. 8 GPa. These data agree with Mössbauer results [14], which indicate a magnetic moment decrease in the same pressure domain.

The first-order nature of the crystallographic and magnetic transitions is well established, as is the non-magnetic state of the hcp phase. Just above the transition different magnetic states are predicted, such as a non-collinear magnetic state or low spin state [5, 11, 16, 17].

This paper reports a combined x-ray absorption spectroscopy (XAS) and x-ray magnetic circular dichroism (XMCD) study of this transition, which highlights the close relationship between the structural transition and the decrease of the magnetic moment. The high sensitivity of XMCD allows us to describe precisely the magnetic transition and to relate it to the local structure [18]. The EXAFS and XMCD data are recorded at the same time: XMCD spectra are combinations of two EXAFS (XANES) spectra measured with different x-ray polarizations and/or with different external applied magnetic field on the sample [19]. Therefore, we can extract from these data the magnetic state and the local structure of iron for each pressure simultaneously. Usually, there are difficulties in reproducing good hydrostatic pressure conditions, explaining the large variation of the pressure transition domain of iron in the literature. This uncertainty affects the absolute value of the transition as well as its extent. Therefore a precise comparison of the crystallographic and magnetic transitions of iron has up to know not been realized because structural and magnetic information were recorded for different samples with different pressure techniques.

2. Experiment

XMCD spectra and XAS were recorded at the ESRF on the dispersive XAS beamline ID24. This station is designed to fulfil the requirements of detecting very small XMCD signals (down to $\sim 10^{-3}$) under pressure at the K edges of 3d transition metals [19].

A 4 h long Fe XMCD spectrum is currently achievable with a significant S/N ratio, where the noise is typically reduced to a few 10^{-5}. Performing XMCD studies on a very small sample

requires a focused beam. On the dispersive XAS station at the ESRF (ID24) the beam spot size is about 50 μm^2 FWHM.

Since the x-ray spot is about five times smaller than the sample, after each pressure change a mapping of the sample is done to ensure that it is always the same part of the sample that is probed. This reduces dramatically the influence of the pressure gradient on the relative pressure value of successive data points in a pressure increase. Of course, this is not the case for the absolute pressure value. Inherent to this pressure calibration technique, the absolute pressure uncertainty is about 1 GPa, but the relative pressure uncertainty of different pressure data points in the same run is 0.1 GPa.

The device used at high pressure is a CuBe diamond anvil cell (DAC). For installation in the gap of a dipole magnet, our cell was reduced to a low dimension cylinder, 50 mm in diameter and 26 mm in height. In our DAC, a gas on a metallic membrane applies the pressure. The ratio of the membrane surface and the top of the diamond surface gives a pressure of few tens of GPa on the sample for a gas pressure of few tens of bars.

The sample (Goodfellow high purity 4 μm iron foil) was inserted into the CuBe diamond anvil cell and placed in a 0.4 T magnetic field parallel to the x-ray beam. Silicone oil was used as the pressure transmitting medium and the pressure was measured with the ruby fluorescence technique. Real time visualization of the XAS spectra allowed us to remove, from the energy range of interest, the parasitic Bragg reflections from the diamond anvils by means of an appropriate rotation of the cell.

In this experiment, each XMCD spectrum was obtained by accumulating 200 XAS spectra with inversion of the applied magnetic field between taking successive spectra. By comparing the first and the last XAS spectra relating to one XMCD acquisition, it was possible to check the structural stability of the sample during the measurement.

3. Results

XMCD spectra were recorded up to 22.4 ± 0.1 GPa (while increasing pressure; no pressure decrease was performed). A total of four runs were carried out on freshly loaded samples, to check the reproducibility of the data. Figure 1 compares the Fe K edge XAS of pure Fe foil in ambient conditions (the bcc phase) to examples of spectra recorded at different pressures, between 10.0 ± 0.1 GPa and 22.4 ± 0.1 GPa.

The energy range diffracted by the polychromator is limited to the XANES region and the first oscillations of the EXAFS domain. The figure shows very clearly that both the electronic structure and the local structure around Fe are drastically modified above 14 GPa: the shoulder at 7116 eV becomes more resolved, the white line drifts towards higher energies (from 7132 to 7134 eV) and becomes less intense, and the frequency of the EXAFS oscillations is drastically reduced. The last three spectra (from 15.4 GPa) correspond to the hcp structure described in [9], as we discuss below.

The EXAFS signature of the different steps of the Fe bcc–hcp transition was already clearly identified by Wang and Ingalls [9] and the bcc to hcp transition was described as a martensitic transition with a slow variation of the relative bcc and hcp phase abundance. In their work, the transition occurred over a broader pressure range than that observed in the present work. This could be attributed to the different conditions of hydrostaticity within the cell, and underlines the difficulty of reproducing the same thermodynamic conditions in different experiments.

The quantitative analysis of the XANES region presents difficulties mainly related to the theoretical approximation in the treatment of the potential and the need for heavy time-consuming algorithms to calculate the absorption cross section in the framework of a full multiple-scattering approach. We have therefore compared our data to full multiple-scattering

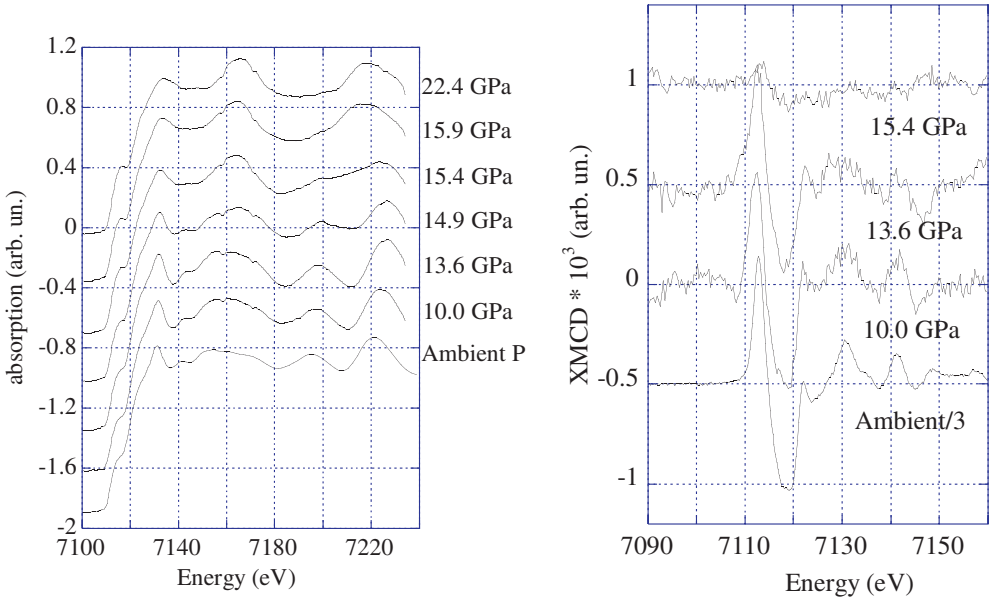

Figure 1. Fe K edge XAS and XMCD as a function of pressure, between the ambient pressure bcc phase and the high pressure hcp phase. The small glitches at 7158 and 7171 eV in the high pressure data are artefacts due to small defects of the polychromator crystal.

calculations using a self-consistent energy dependent exchange–correlation Hedin–Lundqvist potential (FEFF8 package [20]). Self-consistency was obtained by successively calculating the electron density of states, electron density and Fermi level at each stage of the calculation within a 20–25-atom cluster centred on the atom for which the density of states is calculated, and then iterating. Full multiple-scattering XANES calculations were carried out for an 80–100-atom cluster centred on the absorbing atom: all multiple-scattering paths within this cluster were summed to infinite order.

We used the crystallographic parameters of the structurally distorted bcc and hcp phases found in [9] to build the atomic clusters for Fe in the pressure region of the bcc–hcp phase transition. No Debye–Waller-like term was included in the simulations, and this leads to a larger amplitudes of the XAS oscillations compared to experiment.

Figure 2 shows the calculated Fe K edge XANES signal for: (a) the bcc phase at ambient and 11 GPa (full curves bottom); (b) the hcp phase at 14 and 18 GPa (full curves top); and (c) a linear combination of the bcc phase at 11 GPa and the hcp phase at 14 GPa, with coefficients (0.25, 0.75), (0.5, 0.5) and (0.75, 0.25) from bottom to top respectively (dashed curves). Figure 1(a) reports some of the Fe K edge experimental XAS data for comparison.

The ambient pressure bcc cluster is characterized by a first atomic shell of eight atoms at $R \sim 2.48$ Å. This phase is highly compressible, as can be seen from the strong shift towards higher energy of the oscillation at 7220 eV, as pressure is increased to 10 GPa. At this pressure, the first shell has been compressed to $R \sim 2.43$ Å. In the hcp phase described in [9], the first shell is composed of 12 atoms: 6 at ∼2.42 Å and 6 at ∼2.45 Å. The compressibility of this high pressure phase is very low and the local structure remains quasi-identical as P increases from 14 to 18 GPa, as seen from the very small change in the simulated spectra at 14 and 18 GPa.

The phase transition, as depicted in figure 1, is characterized by the following important modifications in the spectra:

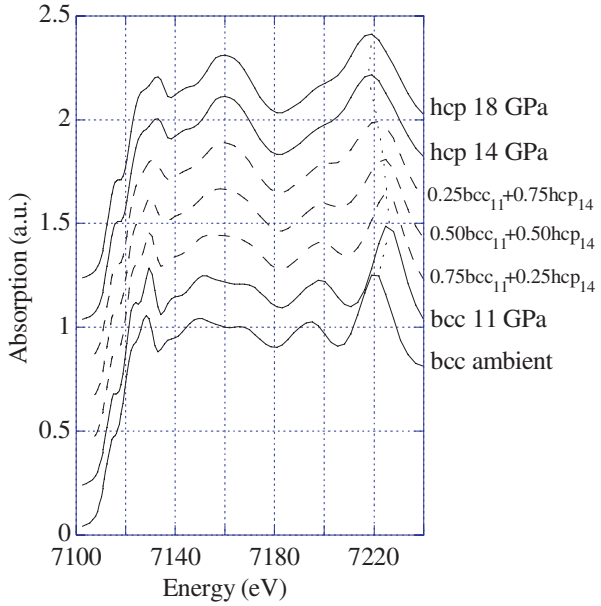

Figure 2. Full multiple-scattering calculations of the Fe K edge XANES signal for: (a) the bcc phase at ambient and 11 GPa (full curves bottom); (b) the hcp phase at 14 and 18 GPa (full curves top); and (c) a linear combination of the bcc phase at 11 GPa and the hcp phase at 14 GPa, with coefficients (0.25, 0.75), (0.5, 0.5) and (0.75, 0.25) from bottom to top respectively (dashed curves).

(1) enhancement of the kink at the onset of the absorption edge, at $E \sim 7116$ eV;
(2) attenuation and shift towards higher energy of the 'white line' feature at $E \sim 7130$ eV;
(3) increase in intensity of the first oscillation, at $E \sim 7160$ eV;
(4) merging of the second and third oscillations;
(5) a peculiar drift of the maximum of the last oscillation towards higher energies (indicating the strong compressibility of the low pressure phase) and then towards lower energies (indicating the mixture of the bcc and hcp phases).

By comparing the simulated XANES spectra in figure 2 with our experimental data in figure 1, we can identify all of these features, and therefore conclude that our XAS data are in agreement with the results of [9], i.e. the phase transition occurs through a gradual variation of the relative bcc and hcp phase abundance. The possible occurrence of intermediate phases, such as the fcc phase suggested in [9], has been tested, but our sensitivity prevents us from reaching a conclusion on this issue, given the important similarity between the fcc (the first shell composed of 12 atoms at 2.43 Å) and the distorted hcp phase (the first shell split into two very close sub-shells).

In order to better identify the onset and the evolution with pressure of the phase transition, we have calculated the first derivative for all XAS spectra close to the transition region, shown in figure 3 for the data between 10 (bottom curve) and 22.4 GPa (top curve). The amplitude of the derivative signal changes drastically between the bcc phase and the hcp phase at the energies marked with a vertical dashed line. It is at these energy points that we have the highest sensitivity to the bcc/hcp phase fraction. The phase fraction calculated from the evolution of the derivatives at the three different energies is identical within the error bar, estimated to be about ± 0.005 from the amplitude of the noise on the derivative signal.

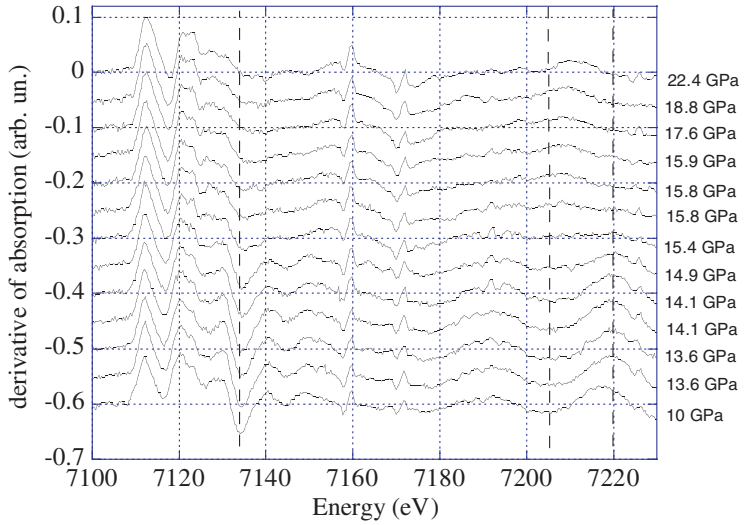

Figure 3. Derivatives of all the absorption spectra, between 10 GPa (bottom curve) and 22.4 GPa (top curve). The data are vertically offset by 0.05 for graphical purposes.

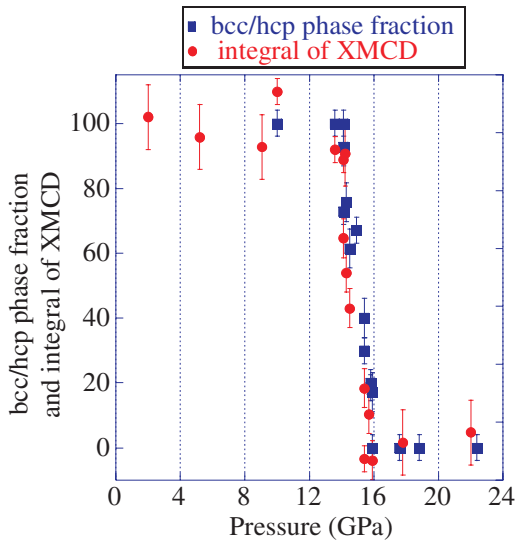

Figure 4. Percentage of bcc phase and integral of the XMCD signal as a function of pressure obtained from the evolution of the amplitude of the derivative signal.

In figure 4 (squares) we plot the evolution of the percentage of bcc as a function of pressure, obtained directly from the evolution of the amplitude of the derivative at these specific energy points.

Figure 4 also shows the pressure dependence of the integral of the XMCD signal (circles). These values are obtained by taking the absolute value of the background-subtracted XMCD signals and integrating over the energy range 7100–7122 eV. The error bar on the integral is estimated from the noise level obtained from the XMCD data. The data in figure 4 derive

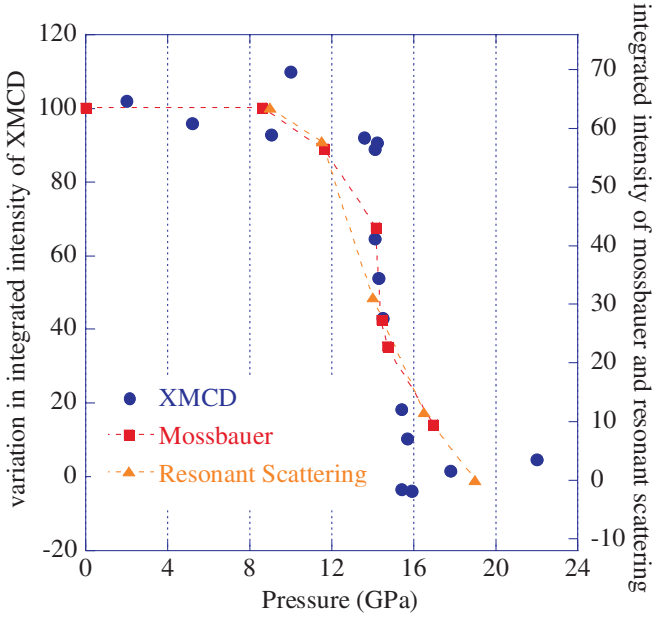

Figure 5. The pressure variation of the integral of the XMCD signal compared with x-ray emission spectroscopy results [15] and Mössbauer spectroscopy [14]. The three methods show the same pressure dependence of the iron magnetic moment, except that our data show a reduced pressure range for the transition.

from three different runs, each characterized by a different noise level related mostly to the homogeneity of the sample. We find that the integral is constant between 0 and 14 GPa within the error bar and decreases abruptly above 14 GPa, when the crystallographic transition starts. The XMCD signal drops to 0 close to 16 GPa. From figure 1 we also see that the pressure increase induces a reduction of the XMCD signal amplitude without any deformation.

In figure 5, our XMCD results are compared to x-ray emission spectroscopy [15] and Mössbauer spectroscopy [14].

4. Discussion

The bcc iron density of states exhibits a large peak in the vicinity of the Fermi level, which is energetically unfavourable [17]. The system lowers its energy by lifting the spin degeneracy, which leads to spin polarization and reduces the density of states at the Fermi level $D(E_F)$. At ambient pressure, the bcc ferromagnetic state is therefore energetically more favourable with respect to the non-magnetic hcp phase.

The effect of pressure is to reduce the inter-atomic distances and therefore to enhance the overlap of the atomic wavefunctions, which broadens the d band and reduces the density of states in the vicinity of the Fermi level. When $D(E_F)$ is small enough, the Stoner criterion is no longer satisfied, and this results in a drop of the magnetic moment and an instability of the bcc phase.

In parallel to this 'magnetic instability', as pressure is increased, any system will have the tendency to transform into denser states of matter ('phonon instability'). For Fe it is however well known that magnetism is able to maintain the low density bcc phase up to at least 10 GPa.

Our data show that between 0 and ∼14 GPa the XMCD signal is constant within the error bar, indicating no sensitive variation of the magnetic moment under pressure when the cell parameter is reduced. The enhancement of the wavefunction overlap induced by the application of pressure below 14 GPa could induce a small magnetic moment decrease, but we do not detect it due to the large error bars.

Between 14 and 16 GPa we observe that the magnetic moment is suddenly reduced to zero. This abrupt drop to zero at the bcc to hcp phase transition proves the first-order nature of the pressure induced magnetic transition, as predicted by Ekman *et al* [17].

Because many of our measurements (XAS and XMCD) are taken simultaneously (no pressure difference between the structural and the magnetic data), our data suggest, from a close look at the transition region in figure 4, that the magnetic transition slightly precedes the structural one. This is in good agreement with the transition pattern given in [17] where theoretical calculations show that the loss of the magnetic moment is at the origin of the structural transition—not the opposite picture where the structural transition results from phonon softening and leads to the loss of magnetic moments. The scenario of a magnetic driven transition is also confirmed by other experimental work on the phonon dispersion of bcc iron up to 10 GPa [21].

The slight discrepancy between magnetic and structural behaviour could also be due to the presence of magnetically dead layers at the interface between the bcc and hcp phase or to the low spin state with an order temperature smaller than room temperature. The importance in the bcc to hcp phase transformation of the shear stresses highlighted by Caspersen *et al* [22] could also be investigated.

In the last part of the transition, just before 16 GPa, the structural transformation is not complete but the XMCD signal is reduced to zero. Here the abundance of the bcc form is very small and its lattice parameter behaves anomalously because it is observed to increase with pressure [9]. This is contradictory with a decreasing magnetic moment, because an increasing lattice constant should lead to a narrowing of the 3d band and to a larger magnetic moment. It is therefore questionable to consider the remaining part of the iron, which is not yet hcp as still being bcc. Since the iron bcc to hcp transition is a martensitic transition (i.e. the newly formed hcp phase is derived form the initial one via collective shear movements of atomic planes), the two phases have coherent interfaces. Towards the end of the transition, when the hcp phase abundance is large, the interfacial strain can lead to anomalous structures in the remaining part of non-hcp phase, which can be seen as an intermediate phase and does not give rise to any XMCD signal.

In [17], the authors report a theoretical prediction of a high spin to low spin transition with intermediate magnetic moments of about 1 μ_B in such an intermediate phase. The coordination number changes during the transition from the bcc magnetic phase with eight nearest and six next nearest neighbours to the hcp non-magnetic phase with 12 nearest neighbours. In an intermediate phase with the coordination number of 10 + 2 a stabilization of intermediate magnetic states is possible.

We do not have any experimental evidence for an intermediate low spin state at pressures higher than 16 GPa, where a region of non-hcp phase can still exist, even if it is not detectable in our XAS data. We cannot conclude here that intermediate spin states are absent, because a reduced XMCD signal could originate from a non-magnetic state, an antiferromagnetic state or a ferromagnetic order temperature lower than the experimental one.

This could explain the discrepancy between our XMCD results and the x-ray scattering and Mössbauer results (figure 5) at pressures above 16 GPa. Nevertheless, the uncertainty of these two last methods prevents us from reaching a conclusion on whether any ferromagnetic or paramagnetic phase is still present above 16 GPa. Moreover, these two

last methods do not allow precise control of the complete achievement of the structural transition.

The observed absence of macroscopic magnetization is in good agreement with the recent observation of the onset of superconductivity in iron above 15 GPa and below 2 K, which is not compatible with a ferromagnetic state [10]. Superconductivity in iron appears only in the pure hcp phase above 15 GPa. Very recently, the presence of magnetic fluctuations in pure hcp Fe has been reported as a possible origin of the superconductivity [23, 24]. These fluctuations in hcp are found to be incommensurate antiferromagnetic at low temperature and are not compatible with a remaining ferromagnetic order or a non-collinear magnetic state.

In the future we hope to reproduce this experiment at low temperatures with a larger XAS energy domain to look for any such intermediate phase. Moreover, it would be interesting to perform both pressure increase and decrease studies in an effort to achieve full understanding of the origin of the mismatch between the two transitions (magnetic and structural).

5. Conclusions

XAS and XMCD measurements performed simultaneously on a sample in particular thermodynamic conditions, such as at high pressure or/and high or low temperature, constitute a powerful tool for correlating changes in structural and magnetic properties. When these changes occur in a very narrow domain, such correlation cannot be determined by measurements on different samples because of the difficulties in reproducing exactly the same thermodynamic conditions.

We have measured the XAS and XMCD signal of iron metal under pressure along the bcc to hcp phase transition. The local structural transition occurs within 2.4 ± 0.2 GPa and the magnetic one within 2.2 ± 0.2 GPa [18]. These are much sharper than those usually described in the literature. The magnetic transition seems to slightly precede the structural one, suggesting that the loss of the magnetic moment lies at the origin of the structural transition.

We plan to develop in the future low temperature XMCD measurements combined with XAS in a larger energy domain to identify more precisely the structural and magnetic structure of the high pressure phase just above 16 GPa during the pressure increase.

References

[1] Brouder Ch and Hikam M 1991 *Phys. Rev.* B **43** 3809
[2] Igarachi J and Hirai K 1994 *Phys. Rev.* B **50** 17820
Igarachi J and Hirai K 1996 *Phys. Rev.* B **53** 6442
[3] Ankudinov A L and Rehr J J 1997 *Phys. Rev.* B **56** R1712
[4] Hasegawa H and Pettifor D G 1983 *Phys. Rev. Lett.* **50** 130
[5] Stixrude L, Cohen R E and Singh D J 1994 *Phys. Rev.* B **50** 6442
[6] Jeanloz R 1990 *Annu. Rev. Earth Planet Sci.* **18** 357
[7] Bancroft D, Peterson E L and Minshall S 1956 *J. Appl. Phys.* **27** 291
[8] Nicol M and Jura G 1963 *Science* **141** 1035
[9] Wang F M and Ingalls R 1998 *Phys. Rev.* B **57** 5647
[10] Shimizu K, Kimura T, Furomoto S, Takeda K, Kontani K, Onuki Y and Amaya K 2001 *Nature* **412** 316
[11] Bose S K, Dolgov O V, Kortus J, Jepsen O and Andersen O K 2003 *Phys. Rev.* B **67** 214518
[12] Cort G, Taylor R D and Willis J O 1982 *J. Appl. Phys.* **53** 2064
[13] Taylor R D, Cort G and Willis J O 1982 *J. Appl. Phys.* **53** 8199
[14] Taylor R D, Pasternak M P and Jeanloz R 1991 *J. Appl. Phys.* **69** 6126
[15] Rueff J P *et al* 1999 *Phys. Rev.* B **60** 14510
[16] Asada T and Terakura K 1992 *Phys. Rev.* B **46** 13599
[17] Ekman M, Sadigh B, Einarsdotter K and Blaha P 1998 *Phys. Rev.* B **58** 5296

[18] Mathon O, Baudelet F, Itié J P, Polian A, d'Astuto M, Chervin J C and Pascarelli S 2004 *Phys. Rev. Lett.* **93** 255503
[19] Mathon O, Baudelet F, Itié J P, Pasternak S, Polian A and Pascarelli S 2004 *J. Synchrotron. Radiat.* **11** 423
[20] Ankudinov A L, Ravel B, Rehr J J and Conradson S D 1998 *Phys. Rev.* B **58** 7565
[21] Klotz S and Braden M 2000 *Phys. Rev. Lett.* **85** 3209
[22] Caspersen K J, Lew A, Ortiz M and Carter E A 2004 *Phys. Rev. Lett.* **93** 115501
[23] Thakor V, Stauton J B, Poulter J, Ostanin S, Ginatempo B and Bruno E 2003 *Phys. Rev.* B **67** 180405 (R)
[24] Saxena S S and Littlewood P B 2001 *Nature* **412** 290